HHS Public Access

Author manuscript

*Ophthalmic Genet*. Author manuscript; available in PMC 2023 June 01.

Published in final edited form as:

*Ophthalmic Genet*. 2022 June ; 43(3): 378–384. doi:10.1080/13816810.2021.2010773.

# A homozygous in-frame duplication within the LRRCT consensus sequence of *CFAP410* causes cone-rod dystrophy, macular staphyloma and short stature

**Ning Chiu**[a], **Winston Lee**[b,c], **Pei-Kang Liu**[c,d,e,f], **Sarah R Levi**[c], **Hung-Hsi Wang**[c], **Nelson Chen**[c], **Eugene Yu-Chuan Kang**[g,h], **Go Hun Seo**[i], **Hane Lee**[i], **Laura Liu**[g,h], **Wei-Chi Wu**[g,h], **Shawn H. Tsai**[a,j,k,*], **Nan-Kai Wang**[c,*]

[a]Department of Ophthalmology, Mackay Memorial Hospital, Taipei, Taiwan

[b]Department of Genetics and Development, Columbia University, New York, New York, USA

[c]Edward S. Harkness Eye Institute, Department of Ophthalmology, Columbia University Irving Medical Center, New York, New York, USA

[d]Department of Ophthalmology, Kaohsiung Medical University Hospital, Kaohsiung Medical University, Kaohsiung, Taiwan

[e]School of Medicine, College of Medicine, Kaohsiung Medical University, Kaohsiung, Taiwan

[f]Institute of Biomedical Sciences, National Sun Yat-sen University, Kaohsiung, Taiwan

[g]College of Medicine, Chang Gung University, Taoyuan, Taiwan

[h]Department of Ophthalmology, Chang Gung Memorial Hospital, Linkou Medical Center, Taoyuan, Taiwan

[i]Division of Medical Genetics, 3billion Inc., Seoul, South Korea

[j]Department of Optometry, Chung Shan Medical University, Taichung, Taiwan

[k]Department of Optometry, Mackay Junior College of Medicine, Nursing, and Management, Taipei, Taiwan

## Abstract

Ciliopathies are a group of genetic dystrophies causing syndromic and non-syndromic retinal degeneration. We identified *CFAP410* as the causative gene in a patient with childhood-onset retinal dystrophy without other systemic symptoms at the age of 20. This 20-year-old man presented with cone-rod dystrophy and *CFAP410* homozygous in-frame duplication variants (c.340_351dup). His clinical features included early subnormal vision, posterior pole staphyloma, and short stature. Unlike the previously reported features of retinal ciliopathy, our patient showed no obvious retinal pigmentation and only a slight hyper-autofluorescent parafoveal ring at the 16-

**CONTACT** Shawn H. Tsai, shawn60tw@gmail.com, Department of Ophthalmology, Mackay Memorial Hospital, No. 92, Sec. 2, Chung Shan North Road, Taipei 10449, Taiwan.

*Shawn H. Tsai and Nan-Kai Wang contribute equally to this article

Disclosure statement

The authors report no conflicts of interest. The authors alone are responsible for the content and writing of this article.

year follow up. This case report aims to characterize the clinical features in a patient with novel, homozygous and likely pathogenic in-frame duplication variants in the *CFAP410* gene. Ultimately, this report will help contribute to the understanding of *CFAP410*-associated ciliopathies.

### Keywords

Ciliopathy; CFAP410; C21orf2; retinal dystrophy; cone-rod dystrophy; short stature; whole exome sequencing

## Introduction

Ciliopathies are a group of disorders caused by several different genes that are involved in the maintenance of cilia (1-3). Some ciliopathies cause non-syndromic retinal degeneration, while others are syndromic, involving retinal degeneration and systemic manifestations involving the brain, kidney, liver, bone, ear, and reproductive organs (2-4). Non-syndromic ciliopathies with isolated retinal dystrophy include Leber's congenital amaurosis (LCA) and X-linked retinitis pigmentosa (XLRP) (3). Syndromic ciliopathies including Bardet–Biedl Syndrome (BBS) (5), Joubert Syndrome (JBTS) (3), Jeune Asphyxiating Thoracic Dystrophy (JATD) (6), and Usher syndrome type 1 (3) have been identified. Typically, the characteristic features of retinal ciliopathy include pigmentary changes within the retina, hyper-autofluorescent rings and decreased autofluorescence signals (7). However, patients with syndromic ciliopathies usually present with relatively earlier and more severe visual deterioration.

The *CFAP410* gene, previously known as *C21orf2*, encodes a ciliary protein localized in the primary cilia of photoreceptors. The CFAP410 protein is consequently associated with ciliary maintenance, formation, and DNA repair (8,9). Pathogenic variation in the *CFAP410* decreases protein stability and affects cytoplasmic localization of CFAP410 protein, leading to photoreceptor dysfunction (9). *CFAP410* variants were identified in patients with Jeune Asphyxiating Thoracic Dystrophy (JATD) and Axial Spondylometaphyseal Dysplasia (Axial SMD) as syndromic ciliopathies (6,10). To further expand the genotypic and clinical spectrum of *CFAP410*-associated disease, we present a long-term follow up assessment of a young boy with retinal degeneration, macular staphyloma and short stature due to a homozygous in-frame duplication of a critical region of the *CFAP410* gene.

## Case report

A 20-year-old man, born to healthy, non-consanguineous parents of Han Chinese/Taiwanese descent, presented with a history of suboptimal vision beginning at 4 years of age. The patient received subsequent ophthalmic examinations over a 16-year interval, and has since never reported difficulty seeing at night time. There was no apparent nystagmus or strabismus. Anterior segment and pupil examinations were unremarkable. At initial presentation, a fundus examination did not show any pigmentary changes. However, retinal examination at the age of 20 revealed a tessellated fundus, retinal pigment epithelium (RPE) mottling around the vascular arcades, and slightly enlarged disc cupping (Figure 1a). At age 10, posterior segment examination revealed a faint hyper-autofluorescence at

the parafoveal region (white arrowheads) and around the vascular arcades in both eyes (Figure 2a). There were no obvious fundus autofluorescence (FAF) abnormalities outside the vascular arcades. Throughout our 16- year follow-up, we did not observe any obvious bone spicule pigmentation, only a slightly increased FAF (Figure 2b) was observed. At age 20, his best corrected visual acuity (BCVA) was 20/32 in both eyes, which remained stable since age 10. Cycloplegic refraction was −6.00 diopters (D) in both eyes. Axial length was 26.01 mm in the right eye and 26.00 mm in the left eye. Spectral domain optical coherence tomography (SD-OCT) revealed decreased thickness in the outer nuclear layer and intermittent disruptions of the ellipsoid zone both inside and outside the fovea (Figure 1b). In addition, mild posterior pole staphyloma was noted in bilateral macular SD-OCT imaging (Figure 1b). Full-field electroretinogram (ERG) testing revealed a cone-rod pattern of degeneration at age 13, and showed further attenuation of the cone and rod responses upon follow-up at age 20 (Figure 3).

Auditory evoked potential (AEP) testing was within normal limits for the patient's age. Electrolytes and renal function tests, including blood urea nitrogen and creatinine, were normal. Hepatic and renal anomalies were not detected. No skeletal abnormalities were detected in Chest X-ray except for short stature (<mean±2 standard deviations). At 20 years old, the patient's body mass index (BMI) was 25 (Body height: 160 cm, body weight: 64 kg). Whole exome sequencing (11) identified a homozygous 12 base pairs (bp) duplication [c.340_351dup (rs1322189782)] in the *CFAP410* gene, which results in an in-frame insertion of 4 amino acids (Thr, Leu, Pro and Arg) at position 117 of the CFAP410 protein. Sanger sequencing in the patient and both parents confirmed these variants in the *CFAP410* gene. (Figure 4). This variant is ultra-rare with an overall MAF of 0.00005319 in the general population and 0.0007372 amongst East Asians among whom it is exclusively found in the gnomAD database (https://gnomad.broadinstitute.org/) (12). It is also predicted to be highly pathogenic by 3 out of 5 functional annotation algorithms for insertion-deletions including DDGI (95.5% probability), SIFT_indels2 (0.826 confidence score) and PROVEAN (score = −13.000).

The variant occurs near the boundary of Exon 4 and Intron 4 situated 22 bp from the strong canonical splice donor; however, it has no putative effect on splicing (SpliceAI Δ score = 0.03) (Table 1). The CFAP410 protein spans 256 amino acid residues that comprises four structural domains—three leucine-rich repeat (LRR) and a downstream leucine-rich repeat C-terminal (LRRCT)—that are of profound functional and evolutionary importance (Figure 5a). While c.340_351dup does not cause a shift in the reading frame during translation, the mutation disrupts a highly conserved consensus sequence in LRRCT, YRxxΦxxxΦPxΦxxLD, which consists of intermittently spaced hydrophobic residues (Φ) flanked by tyrosine (Y) and aspartic acid (D) at each end (Figure 5b).

The precise function of LRRCT in CFAP410 is currently unknown. However, disease-associated missense variants in this domain have been shown to result in decreased expression of the mutant protein in HEK293T cells (9). The LRRCT domain in the crystal structure of U2A' spliceosomal protein assumes an α-helix confirmation that covers or "caps" the C- terminal opening of the LRR superhelix, shielding its hydrophobic core (13). To model the effect of c.340_351dup on this "capping" function, the structures

of normal (WT) and mutant (p.T114_R117dup) human CFAP410 were generated using the Protein Homology/analogY Recognition Engine, version 2.0 (Phyre2) program. A structural region of high confidence (99.9%) spanning the LRR2, LRR3 and LRRCT domains across 119 residues (~46% coverage) were obtained and analyzed. In both the WT and p. T114_R117dup, LRR2 and LRR3 folded into a helicoidal conformation that is consistent with other structural homologues (e.g., U2A' spliceosomal protein). As expected, the LRRCT domain in the WT structure exhibited an α- helical conformation, capping the LRR superhelix (Figure 5c). In the mutant structure, however, the duplicated residues (p.T114_R117dup) formed a disorganized peptide strand exposing the inner hydrophobic core of the LRR superhelix (Figure 5d).

## Methods

All variants and their MAFs were compared to the gnomAD dataset (http://gnomad.broadinstitute.org; accessed May 2021). Possible splicing effects were analyzed using SpliceAI (14). Further functional annotation of variants was carried out with ANNOVAR using pathogenicity scores of DDIG-in (15), MutPred-InDel (16), CADDv.16 (17), SIFT_indels2 (18), and PROVEAN (19). As a general guideline, pathogenic consequences are predicted for variants with scores >20 for CADDv1.6. The pathogenicity threshold for PROVEAN was set at −2.5, which is the maximum separation between deleterious (< −2.5) and neutral (> −2.5) for binary classifications. Homologous sequences of CFAP410 were queried using the protein BLAST program (https://blast.ncbi.nlm.nih.gov/Blast.cgi?PROGRAM=blastp&PAGE_TYPE=BlastSearch&L INK_LOC = blasthome). Generated multiple sequence alignments were then used identify the LRRCT consensus sequence through Consensus Finder (20). Sequence logos were generated with WebLogo3 (21). The predicted structures of human wild-type and mutant CFAP410 were derived using Phyre2v2.0 (22) and corresponding ribbon diagrams were generated using Chimera-1.15 (23).

## Discussion

We reported a 16-year longitudinal assessment of a patient with a homozygous mutation in the *CFAP410* gene, who presented with features of short stature and retinal ciliopathies, including early onset visual decrease without obvious retinal pigmentation. It was identified that the *CFAP410* mutation could influence not only the ocular phenotype but also the systemic phenotype. The primary cilia in both types of photoreceptors (cones and rods) play an important role in phototransduction (4,24-26). The abnormalities of ciliary proteins can result in retinal dystrophy due to photoreceptor degeneration, which is a common disorder in ciliopathies (4). The outer segments of rods and cones are in fact modified cilia that contain densely packed membranous discs loaded with opsin (4). Thus, the *CFAP410* gene encodes a ciliary protein localized to the primary cilium of the photoreceptors related to syndromic or non-syndromic retinal degeneration. The identified *CFAP410* mutations decreased protein stability and affected ciliogenesis, which induced degradation of the photoreceptors. Systemic manifestations can also occur in any organ, including the eye, ear, liver, kidney, bone and brain. Therefore, the mutations in *CFAP410* could result in a retinal dystrophy with syndromic or non-syndromic manifestations (9). Although mutations in

*CFAP410* have been reported in patients with both retinal dystrophy and skeletal anomalies (8), there were no skeletal anomalies except for short stature (<mean±2 standard deviations) observed in our patient.

Patients with retinal ciliopathies usually present with earlier visual symptoms and less retinal pigmentation as compared to typical patients with retinitis pigmentosa at a similar age. Our patient with the *CFAP410* homozygous in-frame duplication variants (c.340_351dup) had clinical features similar to a previous report of a *CFAP410* mutation with early declining vision and posterior pole staphyloma (27). His BCVA remained at 20/32 in both eyes since he was ten, prognostically milder than other patients with *CFAP410* gene mutations reported in literature (6,8,9,27). Furthermore, our patient presented with no obvious retinal pigmentation, which is a common feature in early age ciliopathies. However, the FAF imaging in our patient showed no significant changes over our 16-year follow-up. This finding differs from the unique FAF patterns noted in many retinal ciliopathies, including a parafoveal hyper-FAF ring and a speckled pattern of hypo-FAF foci. Moreover, there was only a slightly increased FAF parafoveal ring noted at 20 years old. At 13 years old, ERG showed severely decreased cone response with 50% reduction in rod responses, whereas the ERG at 20 years old showed nearly extinguished cone and rod responses. Therefore, the ERG results from our patient indicate that this mutation causes a cone-rod dystrophy, whereby the cone cells are affected earlier and more severely than the rod cells. Once, again, we present a novel finding in that many retinal ciliopathies will present as a rod-cone dystrophy, however, here, the *CFAP410* and *RPGRIP1* mutations cause cone-rod dystrophy in retinal ciliopathies (1,28).

In conclusion, we report a clinical case of recessive mutations in the *CFAP410* gene (c.340_351dup), with cone-rod dystrophy, posterior pole staphyloma and short stature. Although our patient presented features characteristic of a retinal ciliopathy (including no obvious retinal pigmentation), there were also some features that differed from the typical retinal ciliopathy phenotype, including mild hyper-FAF parafoveal ring without significant hypo-AF spots, and a cone-rod pattern of degeneration. Overall, ERG testing and SD-OCT imaging revealed significant damage over the 16-year follow-up, which may suggest that this duplication variant leads to a degenerative process. In order to further understand the implications of this duplication, we will need to continue to closely monitor this patient as well as other similar patients.

## Funding

Nan-Kai Wang and his lab are supported by the National Institute of Health R01EY031354, P30EY019007, Vagelos College of Physicians & Surgeons (VP&S) Grants and Gerstner Philanthropies. The content is solely the responsibility of the authors and does not necessarily represent the official views of the National Institutes of Health.

## References

1. Bujakowska KM, Liu Q, Pierce EA. Photoreceptor cilia and retinal ciliopathies. Cold Spring Harb Perspect Biol. 2017 Oct 3;9(10):a028274. doi:10.1101/cshperspect.a028274. [PubMed: 28289063]
2. Hildebrandt F, Benzing T, Katsanis N. Ciliopathies. N Engl J Med. 2011 Apr 21;364(16):1533–43. doi:10.1056/NEJMra1010172. [PubMed: 21506742]

3. Waters AM, Beales PL. Ciliopathies: an expanding disease spectrum. Pediatr Nephrol. 2011 Jul;26(7):1039–56. doi:10.1007/s00467-010-1731-7. [PubMed: 21210154]
4. Shivanna M, Anand M, Chakrabarti S, Khanna H. Ocular ciliopathies: genetic and mechanistic insights into developing therapies. Curr Med Chem. 2019;26(17):3120–31. doi:10.2174/0929867325666180917102557. [PubMed: 30221600]
5. Mockel A, Perdomo Y, Stutzmann F, Letsch J, Marion V, Dollfus H. Retinal dystrophy in Bardet-Biedl syndrome and related syndromic ciliopathies. Prog Retin Eye Res. 2011 Jul;30(4):258–74. doi:10.1016/j.preteyeres.2011.03.001. [PubMed: 21477661]
6. McInerney-Leo AM, Wheeler L, Marshall MS, Anderson LK, Zankl A, Brown MA, Leo PJ, Wicking C, Duncan EL. Homozygous variant in C21orf2 in a case of Jeune syndrome with severe thoracic involvement: extending the phenotypic spectrum. Am J Med Genet A. 2017 Jun;173(6):1698–704. doi:10.1002/ajmg.a.38215. [PubMed: 28422394]
7. Takahashi VKL, Xu CL, Takiuti JT, Apatoff MBL, Duong JK, Mahajan VB, Tsang SH. Comparison of structural progression between ciliopathy and non-ciliopathy associated with autosomal recessive retinitis pigmentosa. Orphanet J Rare Dis. 2019 Aug 1;14 (1):187. doi:10.1186/s13023-019-1163-9. [PubMed: 31370859]
8. Shin DH, Kim AR, Woo HI, Jang JH, Park WY, Kim BJ, Kim SJ. Identification of the CFAP410 pathogenic variants in a korean patient with autosomal recessive retinitis pigmentosa and skeletal anomalies. Korean J Ophthalmol. 2020 Dec;34(6):500–02. doi:10.3341/kjo.2020.0087. [PubMed: 33307614]
9. Suga A, Mizota A, Kato M, Kuniyoshi K, Yoshitake K, Sultan W, Yamazaki M, Shimomura Y, Ikeo K, Tsunoda K, et al. Identification of novel mutations in the LRR-cap domain of C21orf2 in Japanese patients with retinitis pigmentosa and cone–rod dystrophy. Invest Ophthalmol Vis Sci. 2016 Aug 1;57(10):4255–63. doi:10.1167/iovs.16-19450. [PubMed: 27548899]
10. Wang Z, Iida A, Miyake N, Nishiguchi KM, Fujita K, Nakazawa T, Alswaid A, Albalwi MA, Kim O-H, Cho T-J, et al. Axial spondylometaphyseal dysplasia is caused by C21orf2 mutations. PLoS One. 2016;11(3):e0150555. doi:10.1371/journal.pone.0150555. [PubMed: 26974433]
11. Seo GH, Kim T, Choi IH, Park J-Y, Lee J, Kim S, Won D-G, Oh A, Lee Y, Choi J, et al. Diagnostic yield and clinical utility of whole exome sequencing using an automated variant prioritization system, EVIDENCE. Clin Genet 2020 Dec;98(6):562–70. doi:10.1111/cge.13848. [PubMed: 32901917]
12. Karczewski KJ, Francioli LC, Tiao G, Cummings BB, Alfoldi J, Wang Q, Collins RL, Laricchia KM, Ganna A, Birnbaum DP, et al. The mutational constraint spectrum quantified from variation in 141,456 humans. Nature. 2020 May;581(7809):434–43. doi:10.1038/s41586-020-2308-7. [PubMed: 32461654]
13. Price SR, Evans PR, Nagai K. Crystal structure of the spliceosomal U2B”-U2A’ protein complex bound to a fragment of U2 small nuclear RNA. Nature. 1998 Aug 13;394(6694):645–50. doi:10.1038/29234. [PubMed: 9716128]
14. Jaganathan K, Kyriazopoulou Panagiotopoulou S, McRae JF, Darbandi SF, Knowles D, Li YI, Kosmicki JA, Arbelaez J, Cui W, Schwartz GB, et al. Predicting splicing from primary sequence with deep learning. Cell. 2019 Jan 24;176(3):535–48 e24. doi:10.1016/j.cell.2018.12.015. [PubMed: 30661751]
15. Zhao H, Yang Y, Lin H, Zhang X, Mort M, Cooper DN, Liu Y, Zhou Y. DDIG-in: discriminating between disease-associated and neutral non-frameshifting micro-indels. Genome Biol. 2013 Mar 13;14(3):R23. doi:10.1186/gb-2013-14-3-r23. [PubMed: 23497682]
16. Pagel KA, Antaki D, Lian A, Mort M, Cooper DN, Sebat J, Iakoucheva LM, Mooney SD, Radivojac P. Pathogenicity and functional impact of non-frameshifting insertion/deletion variation in the human genome. PLoS Comput Biol. 2019 Jun;15 (6):e1007112. doi:10.1371/journal.pcbi.1007112. [PubMed: 31199787]
17. Kircher M, Witten DM, Jain P, O’Roak BJ, Cooper GM, Shendure J. A general framework for estimating the relative pathogenicity of human genetic variants. Nat Genet. 2014 Mar;46(3):310–15. doi:10.1038/ng.2892. [PubMed: 24487276]
18. Ng PC, Henikoff S. SIFT: predicting amino acid changes that affect protein function. Nucleic Acids Res. 2003 Jul 1;31(13):3812–14. doi:10.1093/nar/gkg509. [PubMed: 12824425]

19. Choi Y, Sims GE, Murphy S, Miller JR, Chan AP. Predicting the functional effect of amino acid substitutions and indels. PLoS One. 2012;7(10):e46688. doi:10.1371/journal.pone.0046688. [PubMed: 23056405]

20. Jones BJ, Kan CNE, Luo C, Kazlauskas RJ. Consensus Finder web tool to predict stabilizing substitutions in proteins. Methods Enzymol. 2020;643:129–48. doi:10.1016/bs.mie.2020.07.010. [PubMed: 32896278]

21. Crooks GE, Hon G, Chandonia JM, Brenner SE. WebLogo: a sequence logo generator. Genome Res. 2004 Jun;14(6):1188–90. doi:10.1101/gr.849004. [PubMed: 15173120]

22. Kelley LA, Mezulis S, Yates CM, Wass MN, Sternberg MJ. The Phyre2 web portal for protein modeling, prediction and analysis. Nat Protoc. 2015 Jun;10(6):845–58. doi:10.1038/nprot.2015.053. [PubMed: 25950237]

23. Pettersen EF, Goddard TD, Huang CC, Couch GS, Greenblatt DM, Meng EC, Ferrin TE. UCSF Chimera–a visualization system for exploratory research and analysis. J Comput Chem. 2004 Oct;25(13):1605–12. doi:10.1002/jcc.20084. [PubMed: 15264254]

24. Adams NA, Awadein A, Toma HS. The retinal ciliopathies. Ophthalmic Genet. 2007 Sep;28(3):113–25. doi:10.1080/13816810701537424. [PubMed: 17896309]

25. Chen HY, Welby E, Li T, Swaroop A. Retinal disease in ciliopathies: recent advances with a focus on stem cell-based therapies. Transl Sci Rare Dis. 2019 Jul 4;4(1–2):97–115. doi:10.3233/TRD-190038. [PubMed: 31763178]

26. Norris DP, Grimes DT. Mouse models of ciliopathies: the state of the art. Dis Model Mech. 2012 May;5(3):299–312. doi:10.1242/dmm.009340. [PubMed: 22566558]

27. Khan AO, Eisenberger T, Nagel-Wolfrum K, Wolfrum U, Bolz HJ. C21orf2 is mutated in recessive early-onset retinal dystrophy with macular staphyloma and encodes a protein that localises to the photoreceptor primary cilium. Br J Ophthalmol. 2015 Dec;99(12):1725–31. doi:10.1136/bjophthalmol-2015-307277. [PubMed: 26294103]

28. Hadalin V, Sustar M, Volk M, Maver A, Sajovic J, Jarc-Vidmar M, Peterlin B, Hawlina M, Fakin A. Cone dystrophy associated with a novel variant in the terminal codon of the RPGR-ORF15. Genes (Basel). 2021 Mar 29;12(4):499. doi:10.3390/genes12040499. [PubMed: 33805381]

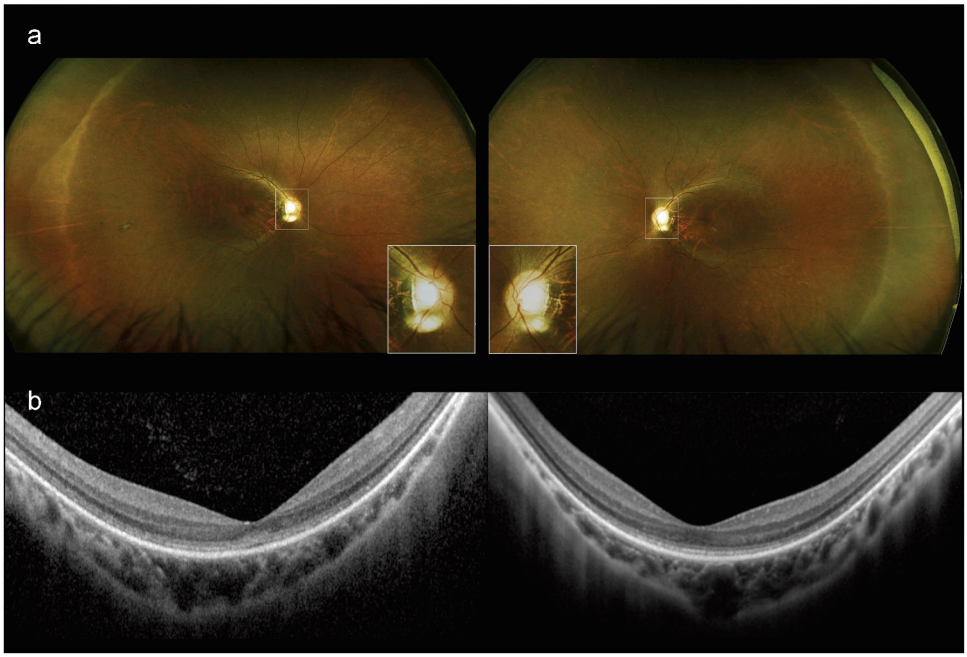


**Figure 1.**

Fundus photography and spectral domain optical coherence tomography (SD-OCT) of patient at the age of 20 (a) Ultrawide-field fundus photographs showed tessellated fundus and RPE mottling around vascular arcade, and slight enlarged disc cupping (small boxes) in both eyes. There was no obvious pigmentation. (b) Horizontal SD-OCT through macular region showed decreased thickness in the outer nuclear layer, ellipsoid zone interruption and loss outside the fovea and posterior pole staphyloma in both eyes.

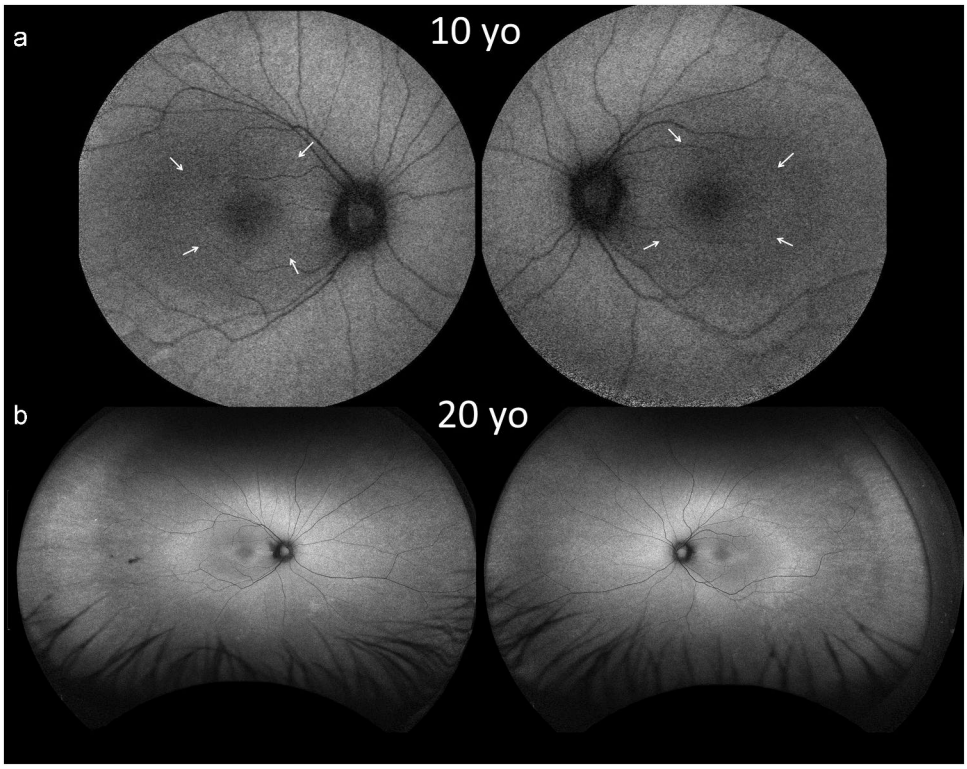


**Figure 2.**

Fundus autofluorescence at age of 10 and 20. (a) Fundus autofluorescence at the age of 10 showed faint hyper autofluorescence at parafoveal region (white arrowheads) and around the vascular arcades in both eyes. (b) Ultrawide-field fundus autofluorescence at the age of 20 showed markedly ring-shaped hyperauto-fluorescence without obvious hypoautofluorescence spots in both eyes.

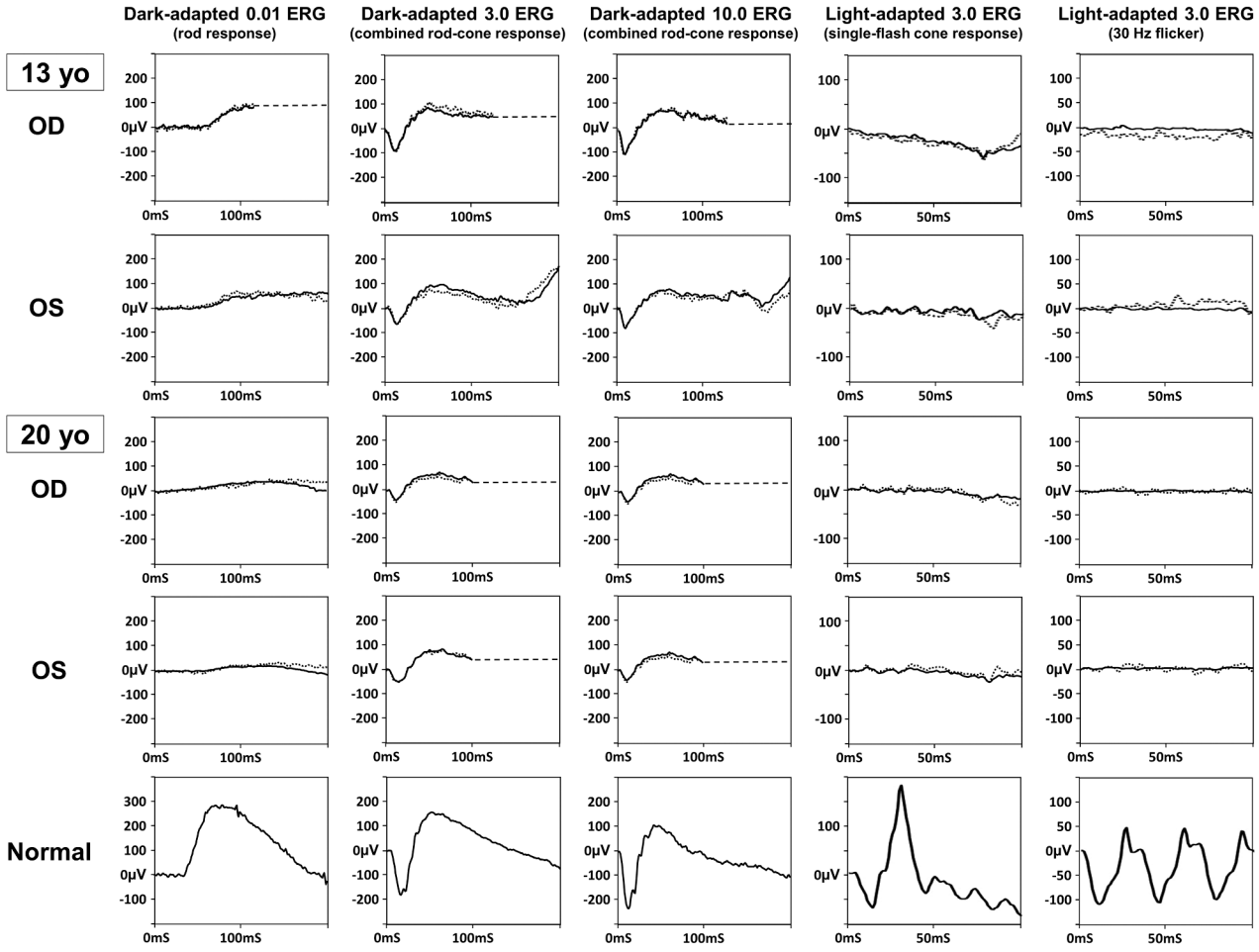


**Figure 3.**

Full-field electroretinogram (ERG). ERG showed severely reduced in cone response with 50% reduction in rod responses at the age of 13. The ERG at 20 years old showed nearly extinguished in both cone and rod responses. (Solid lines represent the average of all tracings, and small dashed lines denote values of a single trace. Long dashed lines represent eye-blink artifacts.)

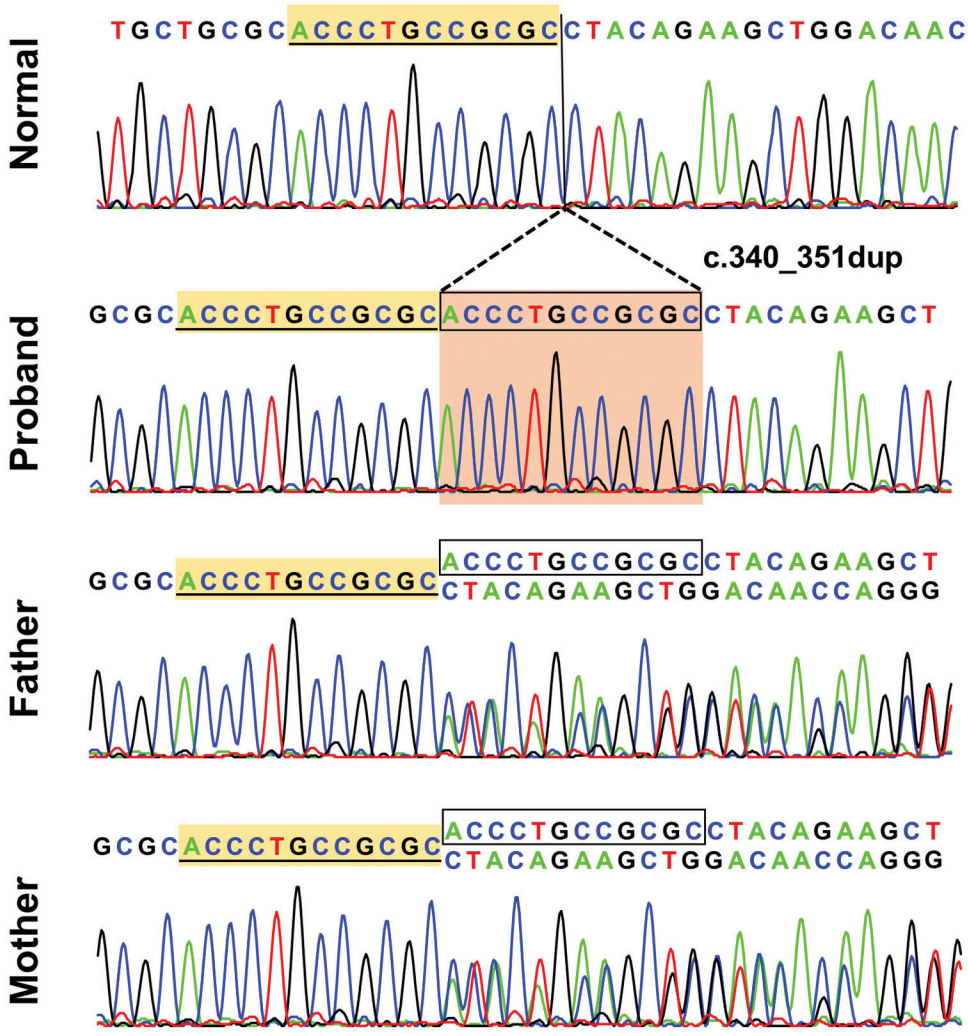


**Figure 4.**

Sanger sequencing of the CFAP410 variant in the patient and his non-consanguineous parents. There is a homozygous variant, c.340_351dup in CFAP410 gene of the patient (highlight in orange background), which causes in-frame p.T114_R117dup. Both parents carry heterozygous variant. There is a homozygous variant, c.340_351dup in CFAP410 gene of the patient (highlight in orange background), which cause in-frame p.T114_R117dup. Both parents carry heterozygous variant.

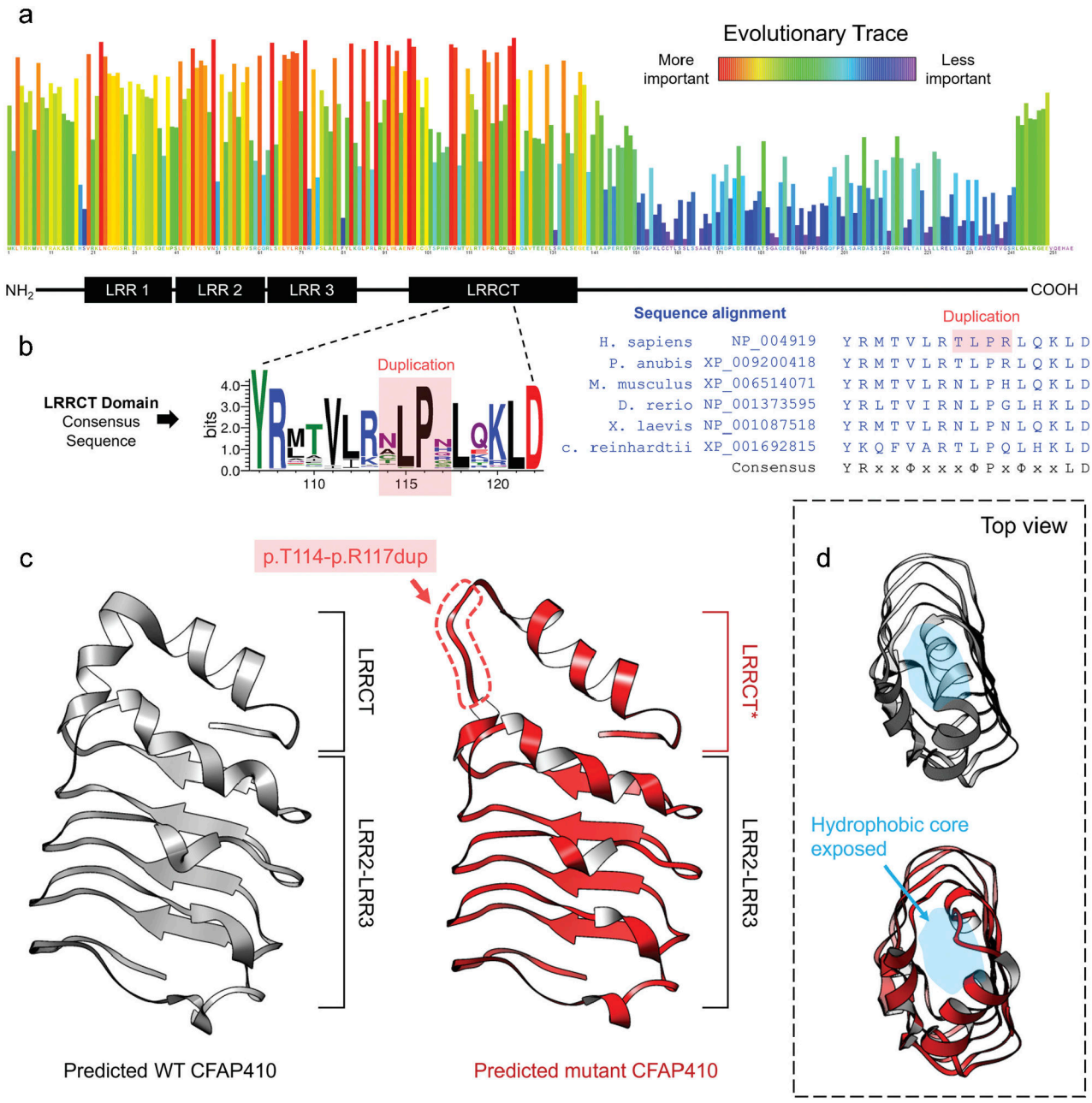


**Figure 5.**

Analysis of identified CFAP410 mutation. (a) The CFAP410 protein spans 256 amino acid residues that comprise known structural domains—3 leucine-rich repeat (LRR) and a downstream leucine-rich repeat C-terminal (LRRCT). (b) The mutation disrupts a highly conserved consensus sequence in LRRCT, YRxxΦxxxΦPxΦxxLD, consisting of intermittently spaced hydrophobic residues (Φ) flanked by tyrosine (Y) and aspartic acid (D) at each end. (c) The LRRCT domain in the WT structure exhibited an α-helical confirmation capping the LRR superhelix. From the top view, the duplicated residues (p.T114_R117dup)

formed a disorganized peptide strand exposing the inner hydrophobic core of the LRR superhelix.

**Table 1.**

Summary of variant details, minor allele frequency and pathogenicity predictions of the homozygous 12 bp insertion identified in the proband.

| **Variant details** | |
|---|---|
| Gene | Cilia And Flagella Associated Protein 410 (*CFAP410*) |
| gDNA (GRCh38) | g.44333055_44333066dup |
| cDNA (NM_001271441.1) | c.340_351dup |
| Protein | p.Thr114_Arg117dup |
| Location | Exon 4 |
| Domain | Leucine rich repeat C-terminal domain (LRRCT) |
| Type | Duplication |
| Coding effect | In-frame |
| dbSNP | rs1322189782 |
| Clinical Significance (ClinVar) | Not reported |
| ACMG/AMP classification | PM4 |
| **Allele frequency (gnomAD v2.1.1)** | |
| Total | 0.00005319 |
| East Asian | 0.0007372 |
| Other populations | Absent |
| Homozygotes | Absent |
| ***In silico*pathogenicity prediction** | |
| DDGI | Pathogenic (95.5% probability) |
| MutPred-InDel | 0.3331 |
| CADDv1.6 | 14.71 |
| Sift Indel | Damaging (0.826 confidence score) |
| PROVEAN | −13.000 (Deleterious) |
| SpliceAI | Donor loss Δ score = 0.03 (−1208 bp) |